

PDF hosted at the Radboud Repository of the Radboud University Nijmegen

The following full text is a publisher's version.

For additional information about this publication click this link.

<http://hdl.handle.net/2066/149140>

Please be advised that this information was generated on 2017-12-05 and may be subject to change.

Percept-choice sequences driven by interrupted ambiguous stimuli: A low-level neural model

A. J. Noest

Functional Neurobiology Department, Helmholtz Institute,
Utrecht University, Utrecht, The Netherlands



R. van Ee

Department Physics of Man, Helmholtz Institute,
Utrecht University, Utrecht, The Netherlands



M. M. Nijs

Functional Neurobiology Department, Helmholtz Institute,
Utrecht University, Utrecht, The Netherlands

R. J. A. van Wezel

Functional Neurobiology Department, Helmholtz Institute,
Utrecht University, Utrecht, The Netherlands



Existing neural explanations of spontaneous percept switching under steady viewing of an ambiguous stimulus do not fit the fact that stimulus interruptions cause the *same* percept to reappear across many ON/OFF cycles. We present a simple neural model that explains the observed behavior and predicts several more complicated percept sequences, without invoking any “high-level” decision making or memory. Percept choice at stimulus onset, which differs fundamentally from standard percept switching, depends crucially on a hitherto neglected interaction between local “shunting” adaptation and a near-threshold neural baseline. Stimulus ON/OFF timing then controls the generation of repeating, alternating, or more complex choice sequences. Our model also explains “priming” versus “habituation” effects on percept choice, reinterprets recent neurophysiological data, and predicts the emergence of hysteresis at the level of percept sequences, with occasional noise-induced sequence “hopping.”

Keywords: visual rivalry, perceptual memory, perceptual choice, neural dynamics

Citation: Noest, A. J., van Ee, R., Nijs, M. M., & van Wezel, R. J. A. (2007). Percept-choice sequences driven by interrupted ambiguous stimuli: A low-level neural model. *Journal of Vision*, 7(8):10, 1–14, <http://journalofvision.org/7/8/10/>, doi:10.1167/7.8.10.

Introduction

How does the visual system choose a specific percept at the onset of ambiguous or conflicting stimuli? Percept switching during continuous viewing (Alais & Blake, 2004; Blake & Logothetis, 2002) can be broadly explained by how neural adaptation and noise eventually disrupt the competitive short-term stabilization of the current percept. However, it is a long-standing challenge (Orbach, Zucker, & Heath, 1963) to find a mechanism that explains how (multisecond) interruptions of an ambiguous stimulus cause the same percept to reappear across many stimulus ON/OFF cycles. Indeed, the first adaptation-based attempt to explain ambiguous percept repetition (Orbach et al., 1963) failed to reconcile such percept repetition with spontaneous percept switching and with the usual opposite-percept “aftereffect” of unambiguous stimuli (aftereffect persistence across interruptions was explained only recently; van de Grind, van der Smagt, & Verstraten, 2004). Later psychophysical work showed that shorter interruptions of ambiguous stimuli replace percept repetition by alternation (Kornmeier & Bach, 2005;

Orbach, Zucker, & Olson, 1966) but that repetition occurs for a wide diversity of stimulus types (Leopold, Wilke, Maier, & Logothetis, 2002) and conditions (Pearson & Clifford, 2004), even when various stimuli are presented as interleaved sequences (Maier, Wilke, Logothetis, & Leopold, 2003). The attribution of percept repetition after long interruptions to “perceptual memory” (Leopold et al., 2002; Maier et al., 2003) conflicts with the occurrence of percept alternation after short interruptions, and attributing both to “pattern completion” (Maloney, Dal Martello, Sahn, & Spillmann, 2005) raises the question: Which specific neural mechanism underlies these phenomena?

We construct a simple neural network model that generates the observed percept-choice sequences (as well as spontaneous percept switching), without any “high-level” decision making or memory. Percept choice and switching prove to be qualitatively different dynamical processes (Guckenheimer & Holmes, 1983), with the choice process probing directly how even a single stage of competing neural representations can show remarkably complex ambiguity-resolution behavior. We show that the percept-choice process depends crucially on a hitherto

neglected, near-threshold interaction effect between the local adaptation mechanism and a small neural baseline. Stimulus ON/OFF timing then controls the existence and stability of repeating, alternating, or more complex choice sequences. Our model also explains the observed “priming” versus “habituation” (Pearson & Clifford, 2005) effects on percept choice and predicts emergent longer timescale phenomena such as hysteresis at the level of percept sequences, with occasional noise-induced “hopping” between sequence types. The stimulus-onset locked dynamics of the fast, early choice process enable neurophysiological tests with crisp time resolution, and our model actually puts such recent results (Kornmeier & Bach, 2005; Krug, 2004) in a new light. We also envisage that attention- or task-related signals may slowly modulate the neural parameters that control the repertoire of choice sequences.

Results

The guiding principle of our approach is to recognize the process of ambiguity resolution as an instance of a class of dynamically equivalent nonlinear processes that occur throughout nature (e.g., Cross & Hohenberg, 1993; Murray, 1990) and that are mathematically well characterized (Cross & Hohenberg, 1993; Guckenheimer & Holmes, 1983): bifurcation of a stable equilibrium (here, the “null” percept during stimulus interruption) into a pair of short-term stable equilibria (the two possible percepts during the ambiguous stimulus), while the pair symmetry is weakly broken by a “slow” variable (the difference in adaptation states). Formally, our problem belongs to the simplest class of codimension-2 bifurcations (Guckenheimer & Holmes, 1983), and much of what we will need stems from Euler’s 1744 analysis (Euler, 1960) of elastic buckling under compression. Our task then becomes to specify and analyze a particularly simple, neurophysiologically viable model that is representative of the huge class of neural networks capable of robustly producing the hitherto unexplained percept-choice dynamics, in addition to the better known percept switching.

Minimal neural model

Several models of percept switching (e.g., Laing & Chow, 2002; Wilson, 2003) use the neural *outputs* as the primary dynamical variables. Given the thresholded sigmoidal shape of neural firing-rate functions, this makes such models blind to a subthreshold side effect of unequal adaptation that we will identify as sufficient for producing all hitherto unexplained percept-choice phenomena. Without this, one would be led to assume much more complicated mechanisms (see the [Appendix](#) for details).

In our approach, neural outputs occur only as sigmoidal transformations $S(H_i)$ of the primary dynamical variables H_i , called “local fields”, which correspond to the percept (i)-related component of the membrane potentials of the neurons that encode the two rivaling percepts, indexed by $i \in \{1, 2\}$. Reducing the fast (timescale $\tau \ll 1$) neural dynamics to one of the simplest forms that captures all the phenomena of interest here, we employ the pair of differential equations

$$\begin{aligned} \tau \partial_t H_i &= X_i - (1 + A_i)H_i + \beta A_i - \gamma S[H_j]; \\ i, j, &\in \{1, 2\}, \quad i \neq j, \end{aligned} \quad (1)$$

which specify how each H_i integrates its (preprocessed) visual input X_i with the “shunting”-type gain control $(1 + A_i)H_i$ that implements adaptation and the subtractive cross-inhibition $\gamma S(H_j)$. The crucial role and meaning of the term βA_i (or its equivalent alternatives) will become clear in the course of our analysis. As adaptation dynamics, we use the simplest possibility, a standard “leaky integrator”

$$\partial_t A_i = -A_i + \alpha S[H_i]. \quad (2)$$

As long as the A_i dynamics timescale (taken as 1) is much slower than the H_i dynamics timescale ($\tau \ll 1$), it does not affect the pattern of our results. Unless stated otherwise, we assume strictly ambiguous inputs $X_i = X$, because we focus on how the system resolves ambiguities based purely on its slowly evolving adaptation levels A_i . Visit [Supplementary Material](#) for Simulink code of a neural network directly matching this form of the model.

Percept choice versus percept switch

The first notable result is the fundamentally different nature of the dynamical process behind percept choice (directly after stimulus onset) compared to spontaneous percept switching (after prolonged viewing): The choice process ([Figure 1a](#)) corresponds to how H_i trajectories that start near the origin (reached during the stimulus interruption) suddenly diverge when approaching the saddle point (aptly named for its combination of stable and unstable directions) that lies between the two coexisting attractors that encode the two potential percepts. Hence, ambiguity resolution is best probed by responses to the onset of ambiguous stimuli. By contrast, a percept switch ([Figure 1b](#)) occurs after prolonged stimulus presentation, when neural adaptation of the current percept representation (here, $A_2 \gg A_1$) has slowly destabilized its own attractor. Shortly before the attractor disappears by fusion with the saddle point, neural noise will make the system escape from the remnant of the attractor, followed by motion toward the opposite percept attractor. As expected, moderate stimulus perturbations (with no correlation or with anticorrelation between the two X_i values) modulate

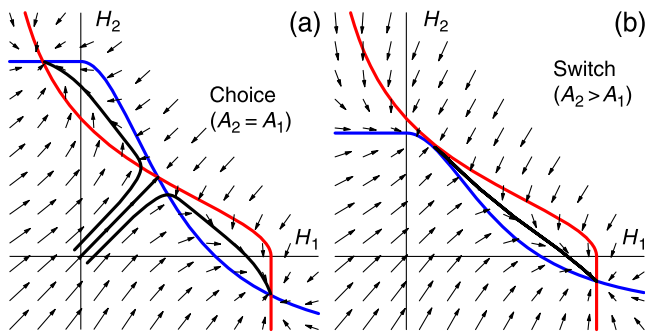


Figure 1. The dynamics of percept choice (a) differs qualitatively from that of a spontaneous percept switch (b): Percept choice is due to divergence of trajectories approaching the saddle point, whereas percept switching is due to adaptation-driven destruction of the currently active attractor (a standard “saddle-node” bifurcation; Guckenheimer & Holmes, 1983). Both panels show (i) the trajectories (black) of the choice or switch events, (ii) the fast-dynamics flow field $\partial_t H_i$ (arrows) defined by Equation 1, (iii) the red (blue) null clines (loci where $\partial_t H_i = 0$) that summarize the crucial, that is, geometric, structure of the H_i dynamics: The saddle point is their on-diagonal intersection in Panel a, and the attractors are their other two intersections (see the Appendix for additional examples).

the timing of each switch event (Kim, Grabowecy, & Suzuki, 2006; Lankheet, 2006), and this can be a rich source of information about how adaptation and noise interact in triggering a percept-switch event. However, it is important to realize that perturbing the percept-switching process probes how bistability is *lost*, not how the neural network can choose systematically between percepts with concurrently stable representations.

Choice alternation or repetition

Focusing on the choice process, the main question becomes what determines the “fate” of trajectories after onset of a fully ambiguous stimulus ($X_1 = X_2$). With symmetric adaptation ($A_1 = A_2$, as in Figure 1a), the fate depends only on whether the (H_1, H_2) state at onset of the stimulus is below or above the diagonal $H_1 = H_2$. Independently of β , the initial (H_1, H_2) is ideally exactly on the diagonal and close to $(0, 0)$, but it is instructive to consider small perturbations of this, which then determine the fate of their trajectories as shown in Figure 1a. One also notices the existence of one special (unstable) trajectory that ends at the saddle point; this special trajectory is key to understanding the choice process in any situation because it forms part of the “separatrix”, the locus that separates all trajectories leading to Percept 1 from those leading to Percept 2. An immediate consequence is that systems without such a separatrix (e.g., Freeman, 2005) do not cover the well-defined percept-choice phenomena we address here.

For asymmetric adaptation (but not so extreme as to destroy one of the attractors), the saddle point and the separatrix attached to it shift leftward and upward when $A_2 > A_1$ and vice versa. Such adaptation asymmetry occurs, for example, when the system was predominantly in one of its attractors before the most recent stimulus interruption. All models that (like our case $\beta = 0$) cannot shift the initial H_i point relative to the separatrix thus predict that the next percept choice is always *opposite* to the previous one, contrary to the observations (Orbach et al., 1963; say, for off-times of more than 1 s). Reduction of adaptation asymmetry has been suggested (Blake, Sobel, & Gilroy, 2003; Chen & He, 2004; Orbach et al., 1963) as a possible cause of percept repetition, but our analysis makes clear that this does not suffice—even small A_i asymmetry in the usual ($\beta = 0$) types of models still predicts choice alternation, and increasing the off-time until the A_i asymmetry decays to the noise level only produces random percept choices. The initial H_i point must be shifted off the diagonal in the same direction as the separatrix is shifted by adaptation asymmetry to allow the previous percept to be chosen—in fact, the initial H_i shift must *overcompensate* for the separatrix shift. Reconsidering the H_i dynamics (Equation 1), one concludes that the model must have $\beta > 0$.

Mathematically, the term βA_i must be in the model simply because it is the lowest order symmetry-allowed term that, even when small, can drive a bifurcation, that is, an addition or deletion of qualitatively different types of system behavior. This standard demand on models is prior to any interpretation of its equations or solutions. In our case, all other formally allowed small changes to the model are found to be either equivalent to β or incapable of driving a bifurcation; thus, leaving all these irrelevant but often “realistic” terms out of the model is safe, and it reduces the analysis to the simplest possible level. Psychophysically, capturing the hitherto unexplained “repetition” choice sequences within the model requires $\beta > 0$, as loosely argued above. The precise dynamical explanation is given in the rest of this article, together with several new predictions. The switching process is not substantially affected by the small β values that explain observed choice sequences.

Neurophysiologically, there are several possible interpretations of a $\beta > 0$ term in the model, which often explain other surprising findings as well. For example, literal translation of both A_i and H_i equations into separate neuron pools yields A_i signaling neurons coupled (with strength β) to the H_i neurons whose gain they down-regulate via shunting inhibition. Such A_i signals explain the hitherto perplexing observation (Leopold & Logothetis, 1996) that many of the neurons that carry percept i signals when driven by unambiguous stimuli, carry a signal with large phase shift relative to percept i dominance when driven by steady ambiguous stimuli (i.e., under spontaneous percept switching, as in Figure 1b): Switching from, say, Percept 2 to Percept 1 corresponds to

A_2 reaching its peak, and this implies that H_2 peaked nearly half a cycle earlier, shortly after Percept 2 started.

Alternatively, a purely formal substitution of the H_i by shifted $h_i \equiv H_i - \beta$ puts our model into the exactly equivalent form

$$\tau \partial_t h_i = X_i - \beta - (1 + A_i)h_i - \gamma S[h_j + \beta], \quad (3)$$

$$\partial_t A_i = -A_i + \alpha S[h_i + \beta]; \quad i, j \in \{1, 2\}, \quad i \neq j. \quad (4)$$

Hence, β can also be interpreted simply as a fixed signal “baseline”. It now performs the same function purely intraneurally (note that this role is now less obvious from the equations), but the existence of phase-shifted neural signals (Leopold & Logothetis, 1996) could still be attributed to separate A_i -carrying neurons. Visit [Supplementary Material](#) for Simulink code of a neural network directly matching this form of the model. More generally, any mixture of the two equivalent model forms and their neural interpretations is equivalent, and this extends to a much wider but precisely delimited range of model variants (see the [Appendix](#)).

In either form, the term parametrized by β interacts with the shunting-type adaptation term $-(1 + A_i)H_i$ to yield offsets $\approx \beta A_i / (1 + A_i)$ in the H_i value at each stimulus onset, relative to their nonadapted values (for details, see the [Appendix](#)). As explained below, it is the size of these A_i -dependent offsets that determines each choice of percept. The fact that their values depend on percept history (via the A_i) will then be shown to explain all known percept-repetition sequences and to predict a host of others. Before we analyze these two temporal scales of choice dynamics, it is worth noting that the crucial H_i shift signals $\approx \beta A_i / (1 + A_i)$ arise from the shunting (or “gain control”) adaptation we use (but if this is present, the effect is not destroyed by common-mode subtractive adaptation, see the [Appendix](#)). Most rivalry models (e.g., Hock, Schöner, & Giese, 2003; Laing & Chow, 2002; Matsuoka, 1984; Wilson, 2003) use purely subtractive adaptation. This leads to the opposite of our predictions because it replaces our product term $(1 + A_i)H_i$ by a linear term of the same form as our βA_i but with a strongly *negative* β value.

Percept-choice dependence on A_i and β

How does the combination of a fixed β with the slowly varying adaptation state (A_1, A_2) determine whether the less adapted or the more adapted attractor is chosen at each stimulus onset? Having identified that the interaction of these factors generates small offsets $\approx \beta A_i / (1 + A_i)$ in the H_i at stimulus onset, one could guess that any (above-noise) difference between these offsets simply gives one of the two H_i a decisive “head start” in the “race” to

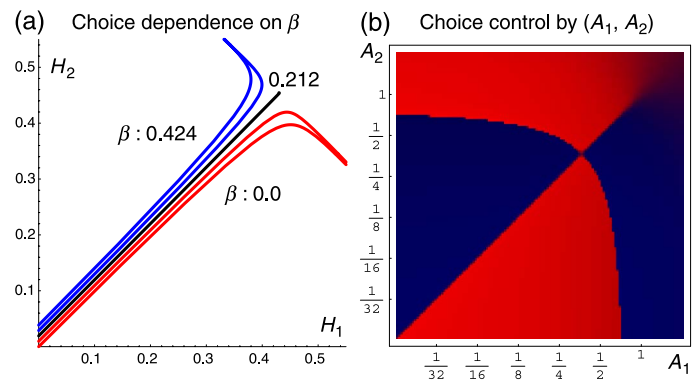


Figure 2. (a) Red/blue trajectories (destined for Percepts 1 and 2) show how the interaction of a finite $\beta > 0$ with any moderate A_i asymmetry (here, $\{A_1, A_2\} = \{0, 0.1\}$) shifts the H_i initial conditions sufficiently (blue) or insufficiently (red) to overcome the A_i asymmetry-induced shift in the saddle point and separatrix (black trace). (b) Red/blue (Percepts 1 and 2) sectors in (A_1, A_2) space show that with a fixed β (here, $\beta = 4/(3\alpha)$) that is large enough to choose the more adapted attractor at low and moderate A_i values (lower left sectors), there are still two upper right sectors at large A_i where the less adapted percept is chosen. This inverted choice regime is essentially due to saturation at large A_i of the shifts $\beta A_i / (1 + A_i)$ in the H_i fixed points, whereas the saddle point continues to shift, eventually annihilating one of the attractors (Figure 1b). The curved boundary between the two sets of sectors shifts to the lower left for smaller β , and it completely disappears for a small $\beta > 0$, as already suggested in Panel a. The crossing of the sector boundaries is, of course, nongeneric under input asymmetry ($X_1 \neq X_2$), such as after unambiguous adaptation of preprocessing stages; this causes the system to produce a normal aftereffect, that is, choice of the least adapted percept (see Figure A2 for details).

dominant activation. Analyzing the actual dynamics of this race leads to less obvious but crucial insights and predictions. The first result, illustrated in Figure 2a, is that β must exceed a finite (but moderate) value before the H_i offset that it creates is sufficient to overcompensate for the shift of the separatrix caused by moderate A_i asymmetry. In psychophysical terms, this “primes” the system to choose the more adapted percept (Pearson & Clifford, 2005; Figure A2 explains how this does not prevent normal aftereffects [van de Grind et al., 2004], that is, choice of the lesser adapted percept [Pearson & Clifford, 2005], when unambiguous stimuli are used to induce adaptation).

The second result is shown in Figure 2b: Given a sufficiently positive β , the choice of the more adapted percept persists in a large but finite regime of adaptation states A_i , the two lower left sectors. However, for very large A_i (upper right pair of sectors), the difference in H_i offsets $\beta A_i / (1 + A_i)$ can no longer surpass the separatrix shift; the system then chooses the less adapted percept.

Choice sequences: Role of ON/OFF timing

In experiments, it will generally be difficult to control the adaptation states A_i directly, especially because any induction of unbalanced adaptation states in the preceding stages destroys the ambiguity of the inputs X_i to the percept-choice network, thereby obliterating the process of interest. The simplest suitable stimulus sequence is a periodic ON/OFF cycle of the same ambiguous stimulus, which allows indirect control over the A_i state at each stimulus onset by means of the T_{ON} and T_{OFF} durations. This is precisely the type of stimulus by which interrupt-induced percept repetition and alternation were discovered (Orbach et al., 1963, 1966). The ensuing choice sequence can then be understood fully in terms of the A_i dynamics during the on and off phases of the cycle—the fast (H_i) dynamics of the percept-choice map shown in Figure 2b acts only at each stimulus onset. This also reduces the choice-relevant A_i dynamics to a discrete-time process, $A_i(t) \rightarrow A_i(t + T_{\text{ON}} + T_{\text{OFF}})$. This (effectively discontinuous) Poincaré map (Guckenheimer & Holmes, 1983) thus contains all information about the existence and stability of all possible choice sequences.

In Figures 3a and 3b, the A_i trajectories are plotted for the two most prominent types of percept-choice sequences that can be produced: For relatively long T_{OFF} (Panel a), the A_i trajectories quickly settle into an attractor that corresponds to repeatedly choosing the same percept, either Percept 1 or Percept 2 depending on the initial condition. For much shorter T_{OFF} (Panel b), the system settles into a sequence of choosing Percept 1 or Percept 2 in alternation. Here, the initial condition merely determines the eventual phase of the percept sequence. For intermediate T_{ON} , T_{OFF} values, the “repeat” and “alternate” attractors coexist, leading to dependence on the initial conditions, to hysteresis, and to noise-induced hopping between the three possible choice sequences (see Figure A4a and its discussion). Panel c shows the (T_{ON} , T_{OFF}) regimes in which various choice-sequence types occur, when using low-adaptation initial conditions. In addition to the repeat and alternation sequences, one may note that, for large T_{ON} , the model also produces sequences with spontaneous percept switches inserted between, and nonlinearly interacting with, the choice events. Given the known highly stochastic timing of percept-switch events (as expected for noisy H_i and/or A_i), these regimes are not optimally probed by regular ON/OFF cycles; hence, we leave their detailed study to another occasion.

Our model makes no assumptions about the specific visual modalities of the stimuli, but it is an open question whether the (hysteretic) transition between various choice-sequence types can be found in all modalities that allow percept-choice dynamics—parameters such as β , which are crucial to percept choice but hardly affect percept switching, may well differ between the neural stages that encode different visual modalities. So far, repeat and

alternation sequences have been reported with certainty only for Necker cubes (Kornmeier & Bach, 2005; Orbach et al., 1966). More diverse experiments and systematic studies of the predicted stimulus timing dependence are clearly called for.

Psychophysical test

As a first exploration, we have tested ambiguously rotating spheres, as well as binocularly rivalrous gratings. The results, summarized in Figure 4, are consistent with the predicted patterns: Broadly speaking, using shorter T_{OFF} intervals tends to replace percept-choice repetition by choice alternation. The crossover T_{OFF} timescale we found is roughly one order of magnitude smaller than the (independently measured) timescale of spontaneous percept switches. The neural adaptation timescale is unknown, but it is probably of the same order of the switching timescale. Thus, our finding of a relatively short T_{OFF} timescale for the coexistence and/or transition zone between percept-repetition and alternation sequences suggests that β is larger than the value used in plotting Figure 3c, although the position and shape of the crossover region depends on all other parameters, including the unknown effective shape of the nonlinearities. The crossover (T_{OFF} , T_{ON}) regimes were roughly overlapping among our four subjects, but the predicted lack of reproducibility due to sequence hysteresis and noise-induced sequence hopping makes precise comparisons difficult. We avoided the long T_{ON} regime where spontaneous switching complicates the dynamics but sampled T_{OFF} down to very small values where temporal blurring of short interruptions begins to make our modeled processes break down (see the Appendix for details).

Discussion

Our model has shown how a rich repertoire of percept-choice behavior emerges from the generic dynamical properties of even a single neural stage of rapidly competing and slowly adapting (proto-)percept representations. The results disprove the need to invoke high-level decision-making or memory processes and provide a coherent set of neural and perceptual predictions for detailed experimental testing.

The local control of each percept choice by neural adaptation has already been tested to some extent, and the results fit our model: Inserting either ambiguous or unambiguous stimulus pulses (Pearson & Clifford, 2005) within interruptions has shown that ambiguous pulses “prime” percept repetition (as we calculate for the long T_{OFF} used), whereas unambiguous pulses reduce percept repetition (the classical aftereffect) by unbalancing the

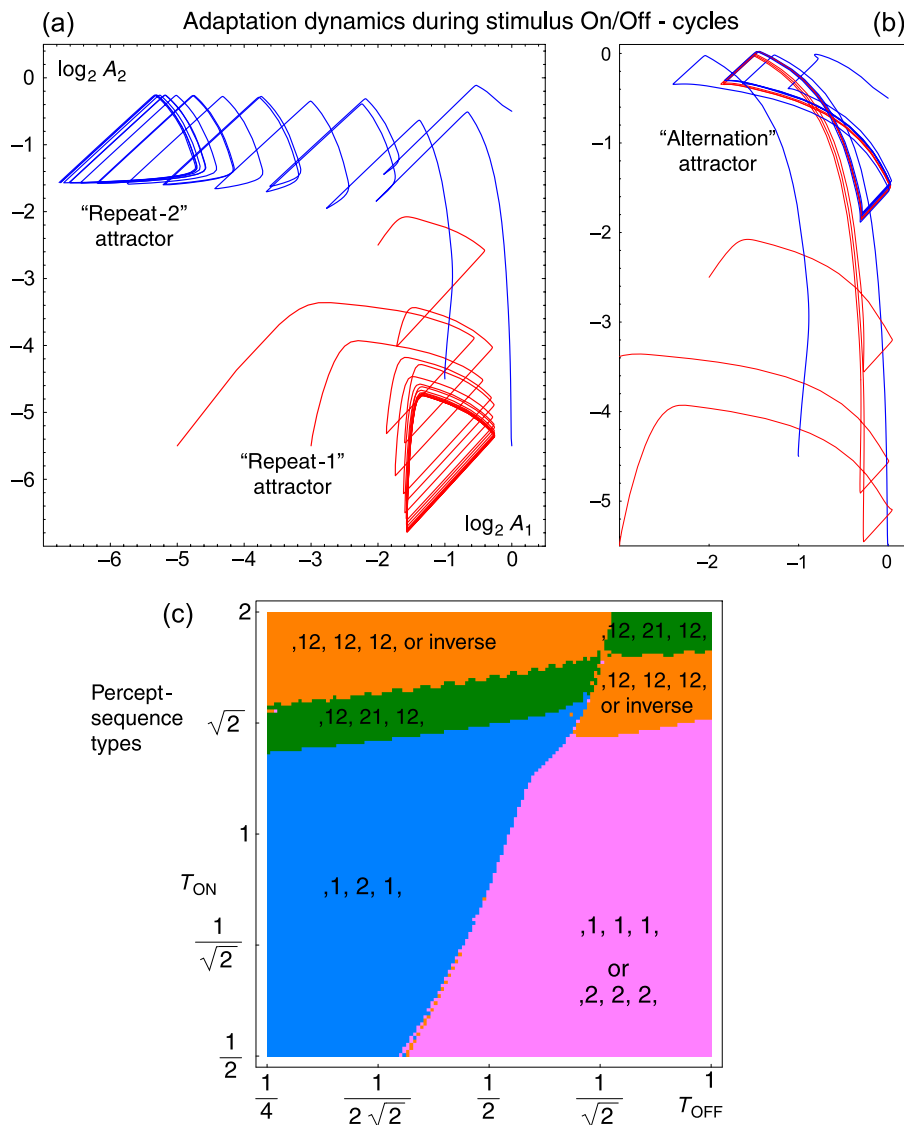


Figure 3. (a and b) Typical A_i trajectories, starting from various initial conditions $A_1 > A_2$, during ambiguous stimulus ON/OFF cycles with T_{ON} , T_{OFF} values such that the percept-choice dynamics are attracted into either the repeat (a) or the alternation (b) type of percept sequence (see Panel c for full sequence classification). The red/blue trace coloring is based on the *initial* A_i values and matches that in Figure 2b. The fast choice (H_i) components of the full network dynamics can still be read from their effect on the A_i dynamics: Each trajectory shows two sharply distinct segments per cycle: During the off-phase, the exponential decay of both A_i shows up as a leftward and downward straight-line segment. During the on-phase, a smoothly curved segment is added. Its shape depends on the percept choice, as decided by the sectors (red/blue) in Figure 2b: In Panel a, with $T_{ON} = 1/2$, $T_{OFF} = 1$, each on-segment shows first the transient of both H_i pair to the saddle point. When the choice is made (here, for a “repeated” percept), the trajectory bends away from the diagonal, as the dominant percept A_i keeps accumulating while the other A_i decays again. Over a few cycles, all trajectories are seen to converge on one of two attractors, corresponding to the “Repeat 1” or “Repeat 2” sequence. In Panel b, with $T_{ON} = 1$, $T_{OFF} = 1/4$, the shorter off-time shows up as shortened straight-line segments. In combination with the longer on-times, this causes the trajectories to leave the repeat sectors in Figure 2b and quickly approach an alternation attractor, common to all trajectories (thus mixing up the red and blue traces). (c) Example of the various percept-choice sequence types (colors) that are produced across (T_{ON}, T_{OFF}) space, in a wide range of initial conditions with low, asymmetric A_i . Sequence types are symbolized with “1” and “2”, labeling the two competing percepts, appearing either alone or in sequential pairs within subsequent on-intervals; commas represent the off-intervals. On- and off-times are in units of the adaptation time constant. Note: These sequence types are generic within the wide class of systems that our model is a particularly simple representative of, but the positions, slopes, and shapes of the regime boundaries depend on all parameters of the model, including its initial conditions, and on the pulse shape of the inputs X_i to our stage, which will actually depend on the impulse responses and adaptation characteristics of all preprocessing stages. Nevertheless, as long as T_{ON} does not allow within-cycle switches, increasing β always favors repetition over alternation, and a larger T_{OFF} will do the same under most conditions. See Figure A4 for the effects of hysteresis and noise.

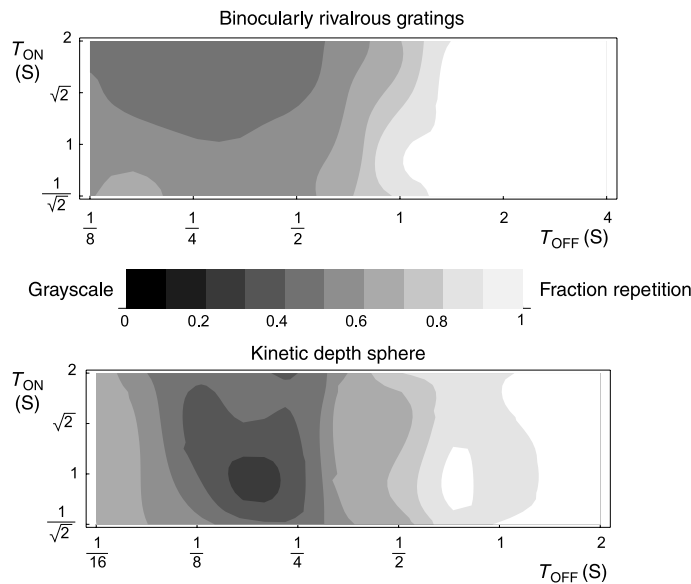


Figure 4. Percentage of “percept repetition”, averaged over four subjects, measured at 44 points in $(T_{\text{OFF}}, T_{\text{ON}})$ space, for very different types of percept competition: binocularly rivalrous gratings (a), and a depth/rotation ambiguous random-dot sphere, rotating about a vertical axis. Statistical errors on the plotted averages are about 10% throughout. Besides the broad pattern (more alternation at small T_{OFF}) that is common to both types of stimuli, one may note the predicted breaking up of measured regime boundaries due to the sequence hysteresis and noise-induced sequence-hopping phenomena that are also characteristic dynamical properties of our model. See the [Appendix](#) for the slight increase in formal repetition probability at very small T_{OFF} .

inputs X_i to our stage through unbalanced adaptation of preceding stages (see [Figure A2](#) for details). Furthermore, the disruption of percept repetition by retinally displacing the stimuli during each interruption (Chen & He, 2004) fits our result that the adaptation states of competing local feature representations are required to enable the dynamics of percept repetition.

Many of our predictions focus on the role of stimulus timing $(T_{\text{OFF}}, T_{\text{ON}})$ as a practical means of influencing the adaptation state of the system at each stimulus onset so that it favors percept repetition or alternation sequences (although this bias is also predicted to show hysteresis and noise effects). An early psychophysical study (Orbach et al., 1966) found some signs that percept repetition breaks down at short T_{OFF} , as we calculate, but studies across several decades since then have focused on the repetition regime (Leopold et al., 2002; Maier et al., 2003; Pearson & Clifford, 2004, 2005)—in the few cases where some percept alternation was reported, it appears to be due at least partly to the insertion of unambiguous stimuli or other perturbations (Chen & He, 2004; Kanai, Moradi, Shimojo, & Verstraten, 2005; Maloney et al., 2005; Pearson & Clifford, 2004, 2005; see also the [Appendix](#)).

Very recently (Kornmeier & Bach, 2005), however, alternating choice sequences evoked by Necker-cube stimuli with short T_{OFF} were used to allow stimulus-locked EEG measurements intended to probe the *switch* process. Our analysis indicates that this experiment, in fact, probes the very different process of percept choice, but this only increases the relevance of this experiment to understanding how the visual system handles actually bistable (rather than temporarily monostable) percept representations. The finding (Kornmeier & Bach, 2005) of occipital choice-related signals at around 100 ms after stimulus onset, well before any response in “higher” stages, strongly supports our theory and contradicts the attribution of the choice process to high-level factors (Leopold et al., 2002; Maier et al., 2003; Maloney et al., 2005).

The stimulus-onset locking of each choice event enables the use of neurophysiological techniques with high time resolution that can probe the nonlinear neural dynamics underlying the choice process. The simple neural structure we have shown to be capable of producing choice sequences can be expected to exist at several stages. The lowest level stage that resolves an ambiguity then prevents subsequent stages from changing the percept sequence. However, a next-level stage may be revealed by dynamically “disabling” the first stage by specifically designed ambiguous stimuli, for example, analogous to the “flicker-and-eyeswitch” stimuli used to probe multilevel percept switching (Pearson & Clifford, 2004; Wilson, 2003).

It would be worthwhile to test more specifically that individual percept-choice events at stimulus onset are causally independent of the neural decision-making (Gold & Shadlen, 2001) processes that undoubtedly occur at higher stages. Indeed, the seemingly “cognitive” ambiguity-resolution abilities of our model could well occur even in the much smaller and simpler neural systems of lower animals, and they should be relatively resistant to moderate levels of anesthesia in higher animals. Note, however, that it is perfectly possible, even likely, that relatively slow top-down signals (encoding, e.g., attention or instruction effects, Ooi & He 1999) can modulate the effective parameters (especially β) that control the stimulus-timing regimes where various choice sequences occur, without deciding each individual percept choice.

Appendix A

Model construction and analysis

Interaction between neural processes with two clearly separate timescales is a crucial ingredient of nearly every theory about perceptual rivalry or ambiguity (Alais & Blake, 2004; Blake & Logothetis, 2002): “fast” cross-inhibition between the neural representations of distinct percepts and a “slow” neural adaptation process. Indeed,

the various forms of these processes implemented in different models (Hock et al., 2003; Kalarickal & Marshall, 2000; Laing & Chow, 2002; Lehky, 1988; Matsuoka, 1984; Wilson, 2003) have all proven capable of broadly reproducing the dynamics of spontaneous perceptual switching, which is usually thought to provide access to the core mechanisms underlying the ability to resolve perceptual ambiguity or conflict. Realizing that switch events only probe how bistability is (temporarily) lost, we set out to find an explicit mechanism that explains the dynamics of choice between actually multistable percept representations.

In the main text, we proposed and analyzed the simplest viable sets of dynamical equations that capture percept choice as well as percept switching. Our explanation of the known choice phenomena (Kornmeier & Bach, 2005; Leopold et al., 2002; Maier et al., 2003; Orbach et al., 1963, 1966; Pearson & Clifford, 2004, 2005), and prediction of new ones, via analysis of this model also identified why and how our model has to differ from all known models. This first fully mechanistic explanation of choice sequences also removes the hitherto perplexing apparent contradiction between percept-choice repetition and the normal aftereffect (van de Grind et al., 2004).

We also pointed out already how two neurophysiologically distinct schemes (in fact, any mixture of these extremes) produce the same dynamical behavior, thus inviting future neurophysiology to find which, if any, of these schemes is actually used. Simulink code for both schemes can be downloaded as [Supplementary Material](#). This allows hands-on experience that may help readers see how the striking neural differences that directly involve the “facilitatory” versus “habituation” effects, which intuitive approaches have aimed to use for explaining percept-choice dynamics, prove to be neither sufficient nor necessary factors and, thus, cannot offer a full mechanistic explanation. As we showed, the explanation becomes clear only via analysis (mostly, the qualitative geometry of attractors, saddle point, and separatrix) that extracts what really matters from the confusingly diverse and rich set of incidental aspects and “confounding factors” that abound in any realization.

Below, we present several more detailed examples and explanations of aspects that we summarized in the main text.

Importance of representing subthreshold states

As mentioned in the main text, using the membrane potentials (H_i or h_i), rather than neural outputs $S(H_i)$, as the primary dynamic variables of the model is not only more realistic but also crucial to discovering that all known percept-choice behavior already emerges from extremely basic, one-stage rivalry models. This result contradicts the long-standing and widely held intuition that the production of percept-repetition choice sequences requires some form of intervention by high-level processes into the low-level neural competition and adaptation

dynamics that we modeled. In terms of explicit mechanisms, it disproves the logical necessity of additional mechanisms or stages or cross-level feedback. The pair of sub-/near-threshold signals parametrized by β (in any of their equivalent forms) play the central role: They enable this simple type of models to describe all the known relevant psychophysics, plus many detailed predictions. In models that take the neural outputs $S(H_i)$ as the primary dynamical variables (e.g., as in Laing & Chow, 2002; Wilson, 2003), subthreshold signals are typically unable to determine the percept choice because, at stimulus onset, both $S(H_i)$ are at or near zero. As illustrated in [Figure A1](#), the observation of adaptation-dependent percept choice then implies that multiple $S(H_i)$ trajectories emerge from the same (nonsingular) starting point, thus proving this type of model to be insufficient.

When staying within the class of $S(H_i)$ -based models, one would thus be forced to attribute this (and other) percept-choice type to other dynamical variables and interactions that, in effect, take control over the neural output dynamics in a manner that must depend on previous output states. This approach has been explored very recently (H. R. Wilson, personal communication), and it appears to require doubling the number of equations, with many more parameters and a specific choice of third-order nonlinearity, so as to implement a two-state “memory” at the synapse level in each of the two competing neural populations. This pair of memory subsystems then controls the $S(H_i)$ dynamics at stimulus onset, producing a roughly similar behavior as emerges from our much simpler and generic H_i -based model. Of course, the brain may actually use even larger complexity, but we favor the simpler explanation until it is refuted by experiment.

Freedom in using variant forms of fast dynamics

The fast-dynamics flow field merely needs to have a geometrically similar structure of null clines intersecting in two attractors and a saddle point (Cross & Hohenberg, 1993; Guckenheimer & Holmes, 1983) as in our simplest example ([Figure 1](#)). This allows a huge class of alternative neural network schemes, far beyond the two types (and any mixture thereof) that we explicitly showed to have identical dynamical behavior. A directly relevant example of this freedom in neurally interpreting the model is that one may take all its dynamical quantities and parameters as representing the corresponding average values over the many millions of neurons and even larger numbers of connections in a one-layer network with two (possibly partly overlapping) competing subsets of neurons and adaptation properties with any of the equivalent structures we identified. More generally, it allows the presence of “fast” interneurons, as have been used in some other models (Wilson, 2003), and even some types of multilayer structure, such as when there is percept-specific cross-inhibitory feedback to lower levels. The fast dynamics and

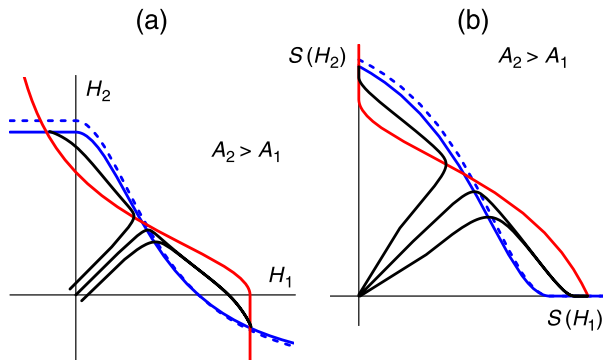


Figure A1. Two views (pre- vs. postsigmoidal signals) of the *same* percept-choice dynamics (given a small excess of Percept 2 adaptation). Both panels show how the (blue, solid line) H_2 null cline for $A_2 > A_1$ is a slightly H_2 -scaled version of the (blue, dashed) null cline for $A_1 = A_2$. This transformation shifts the saddle point, with its attached separatrix, slightly upward and leftward, but Panel a shows that an appropriate small bias in initial (H_1, H_2) state (from any of our β term variants, see Figure 2a) can still make the system choose Percept 2. The right panel shows how the identical dynamics would appear in a model with neural outputs $S(H_i)$ as its dynamical variables: Trajectories with distinct destinations then emerge from the same origin (or indistinguishable ones), thereby disproving such a model and falsely suggesting the necessity of adding specific additional mechanisms to control percept choice. In fact, the converse is true: Our model shows that one only has to uncover the already present subthreshold mechanism from being hidden by the sigmoidal nonlinearity.

fixed-point dimensions of such “intermediate” neurons may be adiabatically eliminated (Cross & Hohenberg, 1993) for the purposes of the “slow” analysis we identified as relevant to understanding how each percept choice is determined by the initial states of the fast part of the network dynamics, which, in turn, is controlled by the interaction of adaptation with β . We now sketch the role of the fast-timescale null clines and fixed points in more detail.

Given fully ambiguous inputs $X_1 = X_2 = X$, the fixed points of the fast-timescale dynamics are determined by the solutions $H_i = H_i^*$ of the two “null cline” equations

$$\partial_t H_i = 0 \Rightarrow H_i(1 + A_i) = X + \beta A_i - \gamma S(H_j) \quad (\text{A1})$$

or their equivalents in terms of $h_i \equiv H_i - \beta$ as dynamical variables

$$h_i(1 + A_i) = X - \beta - \gamma S(h_j + \beta). \quad (\text{A2})$$

As explained in the main text (especially Figure 2), the fate of the percept-choice process depends on (H_1, H_2) at the end of the stimulus interruption. For all but the shortest T_{OFF} (i.e., at least a few times the τ timescale of all stages up to and including the stage[s] modeled here),

this (H_1, H_2) has effectively decayed to the fixed point (H_1^*, H_2^*) for $X = 0$. In this regime, the sigmoidal terms may be neglected; thus, we find $H_i^* \approx \beta A_i / (1 + A_i)$ and $h_i^* \approx -\beta / (1 + A_i)$, respectively. In either form, one notices that (H_1, H_2) acquires A_i -dependent shift components $\approx \beta A_i / (1 + A_i)$ that can compensate (or not, see Figure 2) the oppositely A_i -dependent shift of the separatrix that determines the fate of the trajectory after stimulus onset, that is, the outcome of a percept choice.

Freedom in adding realistic adaptation components

In explaining how percept-repetition sequences arise from the interaction of our $\beta > 0$ term (in any of its forms) with a shunting-type adaptation term such as $(1 + A_i)H_i$, it also became clear that a purely subtractive adaptation mechanism would not allow percept repetition. However, this does not forbid the existence of any subtractive components of adaptation in addition to the required shunting-type component. As expected from the fact that our basic model was the product of keeping only terms with the relevant effect and i, j symmetry, we can freely add back even large *common-mode* subtractive terms (e.g., $-(A_i + A_j)$) without losing any of our original types of model behavior. For example, we find that adding twice as much common-mode subtractive adaptation as our original β term, that is, replacing the fast dynamics by

$$\partial_t H_i = X - (1 + A_i)H_i - \gamma S(H_j) - \beta(A_i + 2A_j), \quad (\text{A3})$$

makes no essential difference to the percept-choice process after trivial recalibrations of some of the parameters (e.g., $\alpha = 6$, $\gamma = 3.5$, $X = 1.3$). Note that with this strong subtractive adaptation component, the effect of any single adaptation change, say, in A_1 , on the local field H_1 is now suppressive instead of stimulatory, that is, *opposite* to what it was in the original model version. This suppressive effect makes the model much more realistic in terms of recordings from individual neurons. However, what is important is that it is of no relevance to how percept choice is produced within the antagonistic neural network and that neurophysiological testing of our choice mechanism is likely to require extracting the small but crucial signals $H_1^* - H_2^*$ from the probably larger but irrelevant common-mode signals.

Sigmoid nonlinearity and coupling parameters

There is a large freedom in specifying the precise form of the sigmoid “firing-rate” function and in the precise value of all parameters because all of the phenomena of interest here are generic under moderate changes in each of these model ingredients. For example, we have verified

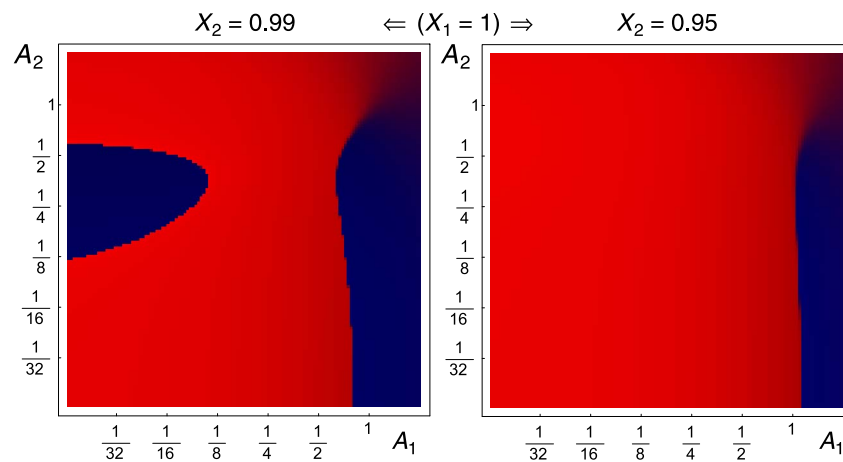


Figure A2. X_i asymmetry can overrule the A_i control of percept repetition (cf. Figure 2). The left panel shows that a 1% difference in the inputs X_i to the modeled stage already causes a significant reduction in the A_i regime where the model chooses the percept (Percept 2, blue) with less stimulus support. For larger X_i asymmetry (right panel), the practically relevant part of this regime vanishes completely—percept choice then simply follows the strongest input (here, Percept 1, red), except when its representation is adapted extremely strongly (blue region at extreme right).

that the same phenomena occur with a wide range of firing-rate nonlinearities, even with the simplest choice that may be viable at the single-cell level, namely, half-wave rectification $S(h) = \max(h, 0)$. Our reason for not using this is that its special feature (piecewise linearity) is not stable under our averaging (Cross & Hohenberg, 1993) over the many neurons that make up a single percept representation. This implies averaging over the neural noise (say, ξ , with some distribution $p(\xi)$), which renormalizes the cell-level firing-rate function, say $s(H)$, to the smooth and suitably generic population-level sigmoid $S(H)$ that appears in the model dynamics:

$$S(H) = \int_{-\infty}^{\infty} s(H + \xi)p(\xi)d\xi. \quad (\text{A4})$$

The same averaging also gets rid of possible differences in the sigmoid shapes between subsets of neurons that contribute to the same percept representation, and similar simplifications emerge with respect to reasonable differences between the adaptation states of individual neurons within the same sets. We note further that changes in the scale and shape of the effective sigmoid $S()$ are largely exchangeable with changes in coupling parameters (e.g., γ , α); what matters is the effects on the gain and/or offset of signals in the fast mutual inhibition feedback loop and/or the slow adaptation loop.

Unbalanced inputs can override A_i -controlled priming

The intersection of sector boundaries in Figure 2 is clearly nongeneric: Any X_i asymmetry will locally “bridge” together a pair of same-colored sectors (red for $X_1 > X_2$) and generally bias the percept choice (see Figure A2). Note

that X_i asymmetry occurs not only when the current stimulus is unbalanced but also when there is “gain” imbalance in the (not bistability-generating) stages preceding the stage we model explicitly. Familiar sources of such gain imbalance are adaptation with unambiguous stimuli or “attention”. This simple mechanism explains how percept-choice repetition can be overridden by a normal aftereffect and how percept repetition is reduced by unambiguous stimuli but enhanced by ambiguous stimuli (Pearson & Clifford, 2005). It also captures how attention can bias the choice process via gain imbalance in the preprocessing and/or the choice-producing stage.

Effect of internal noise and “long-tailed” adaptation

The linear adaptation-decay dynamics used in our basic model suffices for capturing the generation of repeat or alternation sequences in a reasonably wide T_{OFF} regime around where these two types of sequence cross over into another, but it falls short of capturing the known occurrence of reasonably reliable percept repetition for much longer T_{OFF} values. As soon as T_{OFF} exceeds a few times the timescale of the linear adaptation decay we have assumed so far, exponential decay of both A_i will reduce the offsets $\beta A_i/(1 + A_i)$ in the H_i or h_i fixed points that determine the next percept choice. The choice mechanism (which always predicts repetition in this regime) becomes unreliable when the difference between the two $\beta A_i/(1 + A_i)$ terms decays below the effective noise level of the local field (Figure A3)—the actual noise level is unknown, but this affects only logarithmically the maximal T_{OFF} at which reliable percept repetition still occurs, if the A_i decay exponentially.

To allow percept repetition after long off-times, one needs a more realistic, long-tailed adaptation decay

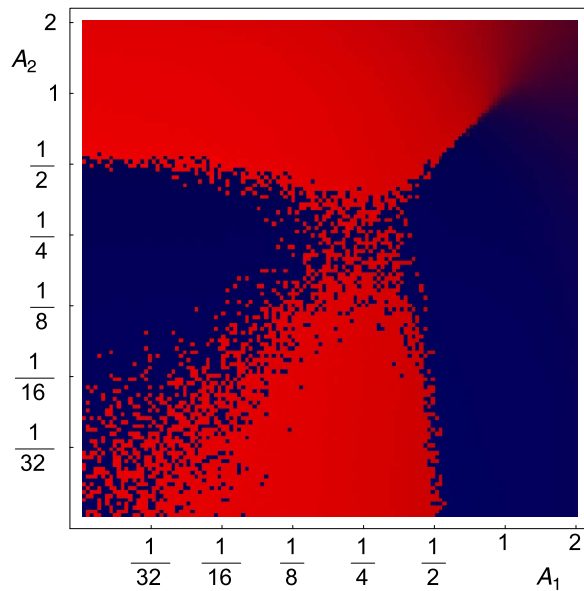


Figure A3. Effect of internal noise on the control of percept choice by the two adaptation signals A_i . For simplicity, this example uses only H_i -level noise (of constant uniformly distributed amplitude, 5×10^{-3} in H_i units, which corresponds to noise at the level of individual neurons that is larger by many orders of magnitude); in reality, there will be noise in the A_i as well, with an amplitude that scales roughly with the square root of the mean value of A_i . Its effect should thus be negligible in the lower left corner of the diagram but could add further scatter along the curved boundary between the red and blue sectors elsewhere. In any event, the diagram illustrates at least qualitatively how (i) in the large A_i regimes, reached only for short T_{OFF} and moderately long T_{ON} , noise blurs the boundary between percept repetition and alternation sequences; and (ii) in the low A_i regimes, reached for large T_{OFF} , the repetition sequence will contain scattered errors that break up the percept sequence into episodes of Repeat 1 and Repeat 2 sequence. As the A_i decay deeply into the noisy regime shown here, the errors become so numerous that the percept-choice sequence becomes almost unpredictable. Existing data (Leopold et al., 2002; Orbach et al., 1963) suggest that this only happens for T_{OFF} values of dozens, perhaps even hundreds, of seconds. This can be explained by the fact that real neural adaptation shows a multi-timescale (Fairhall et al., 2001), long-tailed decay, instead of the simple exponential decay we used in the main text.

instead of an exponential one. Indeed, single-cell recordings have revealed that, already at the retinal stage, adaptation comprises a wide range of timescales, from about 10^{-2} to 10^2 s (Fairhall, Lewen, Bialek, & de Ruyter van Steveninck, 2001). Explicit representation of all the contributing mechanisms, most of which are actually unknown, is not required—the net effect, replacing the usual exponential decay of adaptation by a long-tailed (say, hyperbolic) decay, can be captured most simply by

replacing the linear decay term in the adaptation dynamics by a quadratic term, that is, replacing Equation 2 by

$$\partial_t A_i = -A_i^2 + \alpha S(H_i). \quad (\text{A5})$$

This dynamics may be said to have an adaptation-level-dependent effective timescale $1/A_i$. Its effect on the percept-choice dynamics is small in the small- T_{OFF} regime where the system behavior crosses over from repeat to alternation sequences. This is because large (here, ≈ 1) values of the relevant A_i occur in this regime (see Figure 2), making the effective decay rate (here, A_i) roughly as large as it was in our first linear approximation of the A_i dynamics (Equation 2). The long-tailed adaptation manifests itself at small A_i , thus increasing the longest T_{OFF} values where percept repetition occurs with large probability.

Coexistence of stable sequences and noise-induced attractor hopping

For $X_1 = X_2$, the Repeat 1 and Repeat 2 sequence attractors are equally stable; hence, occasional noise-induced choice “errors” lead to stochastic hopping between these two coexistent sequence attractors. Here, we stress that coexistence (and hopping) occurs also between attractors that are not symmetry related, for example, between the repeat and alternate sequences (see Figure A4a), over a substantial range of timing parameters along regime boundaries such as in Figure 3c. In many experiments, these boundaries will therefore appear as fragmented, irreproducible zones (e.g., as in Figure A4b), and their position will depend on the particular sequence of parameters used (hysteresis). A full analysis of this suprsequence temporal structure is beyond the scope of this article, but we stress the richness of choice-sequence behaviors that emerges from our minimal neural model.

Psychophysical experiment

Methods

Briefly, each run used a 2-min-long regular ON/OFF sequence of stimuli (2° diameter, on a $1,024 \times 768$ pixel, 85-Hz display at 122 cm viewing distance). Subsequent runs sampled the $(T_{\text{OFF}}, T_{\text{ON}})$ plane (up to 44 points) in random sequence, and this sampling was repeated twice per subject. The stimuli (in separate sessions) were (a) a depth/rotation ambiguous sphere, rendered by 40 dots/(deg) 2 , randomly replaced at each stimulus onset, or (b) a binocularly rivalrous dichoptic pair of gratings (orientation, $\pm 45^\circ$; spatial frequency, 1.75 cycles/deg, with a Gaussian envelope of $\sigma = 0.5^\circ$). We asked our four subjects to score percepts during the on-interval, as soon

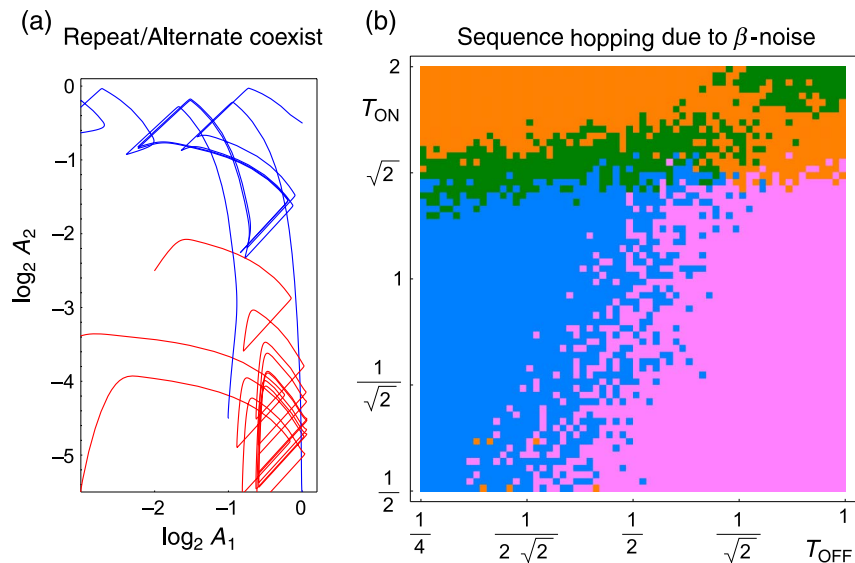


Figure A4. Attractors of various choice sequences can coexist (a), and noise can then make the system hop between these sequences (b). Panel a is similar to Figures 3a and 3b, but with $T_{ON} = 1/\sqrt{2}$ and $T_{OFF} = 1/2$, that is, just right of the boundary between the repeat and alternate regimes shown in Figure 3c. Note that both sequence types attract some of the trajectories, depending on initial conditions. (The boundaries in Figure 3c were computed with low, asymmetric initial A_i , appropriate for most experiments, which favor attraction to the repeat sequences.) Such coexistence implies that most experiments will find different boundaries, depending on the history of stimulus parameters used and on noise perturbations of the A_i state. Panel b shows the same system and initialization as in Figure 3c but with added β noise (SNR = 30 at population level, allowing very much larger neuron-level noise). This (or other) noise causes occasional choice errors, resulting in hopping between sequence attractors that coexist at the stimulus timing used. As illustrated here, this fragments (or, after averaging, blurs) all parameter region boundaries.

as it could be classified as either of the two competing percepts.

Interpretation details

In addition to the main text summary of results and interpretation, we note two subsidiary aspects.

- We avoided sampling the long T_{ON} regime where *spontaneous* percept switching interferes with the onset-locked choice process that we focus on here. The long T_{ON} regime yields interesting but more complicated dynamics, an investigation of which is beyond the scope of this study and, hence, necessitates further research. For the timing conditions used in this study, spontaneous percept switches begin to occur (but remain below 10%), only at the largest on-times (2 s) we tested, and even then, this hardly affected the interruption-locked alternation, as predicted by the top parts of our phase diagram (Figure 3c).
- For very small T_{OFF} (here, roughly $<1/10$ s), temporal smearing by the preprocessing stages prevents X_i from decaying sufficiently close to zero to enable our choice process to occur. This causes a crossover to the slow, spontaneous percept-switching characteristic of uninterrupted ($T_{OFF} = 0$) stimuli. Partial loss of interruption locking at the smallest T_{OFF} registers in our plots as a

formal increase in repetition probabilities. This regime is irrelevant to our model, but it serves to differentiate our *loss* of choice alternation for short T_{OFF} from the recently found (Kanai et al., 2005) *increase* in alternation when a short, strong flash is added to a continuous bistable stimulus: Our T_{OFF} is then about as long as their flashes; thus, the opposite nature of the two effects excludes lumping them as due to some nonspecific effect of stimulus transients. However, if we assume (in line with the proposal of Kanai et al., 2005) that their strong flashes cause temporary ($\approx 1/4$ s) shifts in attention, that is, dips in the neural gain preceding (or within) the stage we model, then this converts the short flashes into effective X_i interruptions with a T_{OFF} for which our model can predict percept alternation. As noted before (Kanai et al., 2005), such assumed gain dips also fit the fact that their flashes can induce temporary disappearance of nonambiguous percepts.

Computational details

Here, we summarize the computational aspects of the results shown in the main-text figures. The choice of parameters and sigmoid shape is such as to produce the percept-choice repertoire that is typical within the wide class of systems that our model is a particularly simple example of. As shown throughout, the existence and

stability of the various types of model behavior differ qualitatively between parameter regimes separated by distinct boundaries (bifurcations), and all our conclusions rest only on these robust patterns.

For definiteness, we used $X = 1$, $\alpha = 5$, $\gamma = 10/3$, $\tau = 1/50$, and sigmoid function $S(z > 0) = z^2/(1 + z^2)$; $S(z \leq 0) = 0$ throughout and chose $\beta = 4/(3\alpha)$ except in plotting the β dependence of the choice dynamics in Figure 2a. All plots were composed by combining the H_i null-cline equations with $H_i(t)$ and $A_i(t)$ trajectories computed by adaptive numerical integration (Mathematica “Dsolve”). In our classification of percept sequences (Figure 3c), the numerical integration for each of 128^2 points in $(T_{\text{OFF}}, T_{\text{ON}})$ space was carried out over the first seven cycles of the stimulus sequence, using the last two on-intervals at each point to determine the sequence types shown. All sequence types shown are stable, and the “run-in” length used suffices for reducing transient-induced errors on the boundary positions to below the plot resolution.

Acknowledgments

This work was supported by a “high potential” grant from Utrecht University, which was jointly awarded to R.v.W. and R.v.E.

Commercial relationships: none.

Corresponding author: Dr. A. J. Noest.

Email: a.j.noest@uu.nl.

Address: Utrecht University, Functional Neurobiology Department, Padualaan 8, NL-3584-CH Utrecht, The Netherlands.

References

- Alais, D., & Blake, R. (Eds.). (2004). *Binocular rivalry*. Cambridge, USA: MIT Press.
- Blake, R., & Logothetis, N. K. (2002). Visual competition. *Nature Reviews Neuroscience*, *3*, 13–21. [PubMed]
- Blake, R., Sobel, K. V., & Gilroy, L. A. (2003). Visual motion retards alternations between conflicting perceptual interpretations. *Neuron*, *39*, 869–878. [PubMed] [Article]
- Chen, X., & He, S. (2004). Local factors determine the stabilization of monocular ambiguous or binocular rivalry stimuli. *Current Biology*, *14*, 1013–1017. [PubMed] [Article]
- Cross, M. C., & Hohenberg, P. C. (1993). Pattern formation outside of equilibrium. *Reviews of Modern Physics*, *65*, 851.
- Euler, L. (1960). Additamentum I de Curvis elasticis; Methodus inveniendi lineas curvas maximi minimi proprietate gaudentes (1744). In Euler Committee of the Swiss Academy of Sciences (Ed.), *Opera Omnia I* (vol. 24, pp. 231–297). Füssli, Zürich. Available at <http://www.math.dartmouth.edu/~euler/>
- Fairhall, A. L., Lewen, G. D., Bialek, W., & de Ruyter van Steveninck, R. R. (2001). Efficiency and ambiguity in an adaptive neural code. *Nature*, *412*, 787–792. [PubMed]
- Freeman, A. W. (2005). Multistage model for binocular rivalry. *Journal of Neurophysiology*, *94*, 4412–4420. [PubMed] [Article]
- Gold, J. I., & Shadlen, M. N. (2001). Neural computations that underlie decisions about sensory stimuli. *Trends in Cognitive Sciences*, *5*, 10–16. [PubMed]
- Guckenheimer, J., & Holmes, P. (1983). *Nonlinear oscillations, dynamical systems, and bifurcations of vector fields*. New York: Springer-Verlag.
- Hock, H. S., Schöner, G., & Giese, M. (2003). The dynamical foundations of motion pattern formation: Stability, selective adaptation, and perceptual continuity. *Perception & Psychophysics*, *65*, 429–457. [PubMed]
- Kalarickal, G. J., & Marshall, J. A. (2000). Neural model of temporal and stochastic properties of binocular rivalry. *Neurocomputing*, *32–33*, 843.
- Kanai, R., Moradi, F., Shimojo, S., & Verstraten, F. A. (2005). Perceptual alternations induced by visual transients. *Perception*, *34*, 803–822. [PubMed]
- Kim, Y.J., Grabowecky, M., & Suzuki, S. (2006). Stochastic resonance in binocular rivalry. *Vision Research*, *46*, 392–406. [PubMed]
- Kornmeier, J., & Bach, M. (2005). The Necker cube—An ambiguous figure disambiguated in early visual processing. *Vision Research*, *45*, 955–960. [PubMed]
- Krug, K. (2004). A common neuronal code for perceptual processes in visual cortex? Comparing choice and attentional correlates in V5/MT. *Philosophical Transactions of the Royal Society of London Series B: Biological Sciences*, *359*, 929–941. [PubMed] [Article]
- Laing, C. R., & Chow, C. C. (2002). A spiking neuron model for binocular rivalry. *Journal of Computational Neuroscience*, *12*, 39–53. [PubMed]
- Lankheet, M. J. (2006). Unravelling adaptation and mutual inhibition in perceptual rivalry. *Journal of Vision*, *6*(4):1, 304–310, <http://journalofvision.org/6/4/1/>, doi:10.1167/6.4.1. [PubMed] [Article]
- Lehky, S. R. (1988). An astable multivibrator model of binocular rivalry. *Perception*, *17*, 215–228. [PubMed]
- Leopold, D. A., & Logothetis, N. K. (1996). Activity changes in early visual cortex reflect monkeys’ percepts during binocular rivalry. *Nature*, *379*, 549–553. [PubMed]

- Leopold, D. A., Wilke, M., Maier, A., & Logothetis, N. K. (2002). Stable perception of visually ambiguous patterns. *Nature Neuroscience*, *5*, 605–609. [PubMed]
- Maier, A., Wilke, M., Logothetis, N. K., & Leopold, D. A. (2003). Perception of temporally interleaved ambiguous patterns. *Current Biology*, *13*, 1076–1085. [PubMed] [Article]
- Maloney, L. T., Dal Martello, M. F., Sahm, C., & Spillmann, L. (2005). Past trials influence perception of ambiguous motion quartets through pattern completion. *Proceedings of the National Academy of Sciences of the United States of America*, *102*, 3164–3169. [PubMed] [Article]
- Matsuoka, K. (1984). The dynamic model of binocular rivalry. *Biological Cybernetics*, *49*, 201–208. [PubMed]
- Murray, J. D. (1990). *Mathematical biology*. Berlin: Springer-Verlag.
- Ooi, T. L., & He, Z. J. (1999). Binocular rivalry and visual awareness: The role of attention. *Perception*, *28*, 551–574. [PubMed]
- Orbach, J., Zucker, E., & Heath, H. A. (1963). Reversibility of the Necker cube. I. An examination of the concept of “satiation of orientation”. *Perceptual and Motor Skills*, *17*, 439–458. [PubMed]
- Orbach, J., Zucker, E., & Olson, R. (1966). Reversibility of the Necker cube: VII. Reversal rate as a function of figure-on and figure-off durations. *Perceptual and Motor Skills*, *22*, 615.
- Pearson, J., & Clifford, C. G. (2004). Determinants of visual awareness following interruptions during rivalry. *Journal of Vision*, *4*(3):6, 196–202, <http://journalofvision.org/4/3/6/>, doi:10.1167/4.3.6. [PubMed] [Article]
- Pearson, J., & Clifford, C. W. (2005). Mechanisms selectively engaged in rivalry: Normal vision habituates, rivalrous vision primes. *Vision Research*, *45*, 707–714. [PubMed]
- van de Grind, W. A., van der Smagt, M. J., & Verstraten, F. A. (2004). Storage for free: A surprising property of a simple gain-control model of motion aftereffects. *Vision Research*, *44*, 2269–2284. [PubMed]
- Wilson, H. R. (2003). Computational evidence for a rivalry hierarchy in vision. *Proceedings of the National Academy of Sciences of the United States of America*, *100*, 14499–14503. [PubMed] [Article]